A Computational Vision Model-based Method to Address Work Zone Conspicuity

Jay E. Barton, James A. Misener, Theodore E. Cohn
California PATH
Institute of Transportation Studies, University of California at Berkeley
Richmond Field Station
1357 S. 46th Street, Bldg 452
Richmond, CA 94804-4698
Phone: 510-231-9465
Fax: 510-231-9565
Email: jebarton@uclink4.berkeley.edu

Abstract. A computational means to assess the conspicuity of highway features was developed, verified, then applied to a sample construction work zone scene. This work was conceived as a balance between modeling the complex phenomena within the human visual system and the need for a simple applications-oriented tool for practitioners to derive a quantitative relative assessment of real world construction work zones in order to rank choices in terms of conspicuity. The results indicate that our vision model-based tool can assess the relative conspicuity of individual elements of a roadway or roadside scene and is relatively straightforward in use. As such, it holds potential value in engaging in "virtual" prototyping of work zone sight lines, colors, and placement of hazard warning cues such as cones, markings and reflective vests.

A Computational Vision Model-based Method to Address Work Zone Conspicuity

Jay E. Barton, James A. Misener, Theodore E. Cohn
California PATH
Institute of Transportation Studies, University of California at Berkeley
Richmond Field Station
1357 S. 46th Street, Bldg 452
Richmond, CA 94804-4698
Phone: 510-231-9465
Fax: 510-231-9565
Email: jebarton@uclink4.berkeley.edu

1. BACKGROUND

1.1 Motivation and Introduction

The primary goal of the work we present in this paper is to develop a cost-effective and usable, yet quantitative and rigorous method and computer tool to evaluate roadside conspicuity. Our intent is that transportation safety practitioners – and even the construction crew – would be able to implement this tool as an objective means of making work zones more conspicuous to approaching drivers. Therefore, short run-time is a necessary goal for the tool. However, a short run-time requirement imposes simplification to the modeling process. The resulting middle ground, a relatively simple to use and reasonable accurate computer tool, is therefore our objective.

It may be appreciated that light measurement per se, such as with simple photometry, is not capable of revealing what we want to learn about the conspicuity of elements in a scene. This is because light measurement only takes account of one type of idiosyncrasy of human vision, that different wavelengths are seen with different efficiencies. Contrast, the ratio of light between adjacent locations, times, or even colors is what the human visual nervous system is computing. In order to emulate that characteristic, a computation that goes well beyond that of photometry must be employed.

In the end, a user with no special expertise in vision modeling should be able to perform a quick "virtual prototype", in which drivers' potential perception of increased conspicuousness could be gauged. In this manner, notional designs and configurations could be quickly simulated under different site lines, color/illumination combinations and ambient lighting conditions.

In this paper we describe the development, validation and application of a computational vision model focused on work zone safety. We begin by an overview of vision modeling taken from two perspectives – as recently theorized by vision science researchers, and as applied in safety studies by transportation researchers. We then describe the development and validation of an intermediate approach, aimed at combining the two perspectives. We illustrate the application of this approach on a roadway scene, and we conclude with a discussion on how this work could be extended to take advantage of its near real time performance.

1.2 Computational Vision Models

1.2.1 Models From Vision Science

There exist in-depth models of early vision, e.g.Visually-Guided Threats (VGT) model by Doll [1] and the Visual Performance Model (VPM) by Witus [2,3]. However, they do not meet our aforementioned ease-of-use and quick run-time criteria. They simulate the complex sequence of events of preattentive vision and human reasoning within the human visual/detection system. Hence, they are intricate in construction; they combine mathematical models post-receptor chromatic-achromatic independence, visual multiplexing, texture perception models, and post-processing based on the Theory of Signal Detection (TSD).

The common sequence of perception computations for VGT and VPM is:

- digitize color video image or independent frames to represent composite macular/peripheral scene images, within the gamut limitations of capturing "true color";
- temporally filter these images into three component images: sustained (lowpass), transient (mid-frequency bandpass) and highly transient (high-frequency bandpass);
- separate color and luminance into five channels (black-white, or luminance only, for each temporal segment, and -- because human color-opponent channels are insensitive to transients -- red-green and yellow-blue channels for the lowpass segment only);
- transform separated color-opponent and luminance images into nine pseudo-images in two dimensional frequency space, with center frequencies spaced at one octave intervals; and
- perform horizontal and vertical orientation filtering on each image.

The resultant images (nominally, 5 color-opponent images x 9 frequency space images x 2 image orientations) are disaggregated by temporal, luminance, color-opponent, spatial and orientation characteristics. These can be directly analyzed in a conspicuousness design sense for spatial energies (for likely detection features) and interchannel covariance (for phase information and, therefore, interrelated edge-detection design attributes). To complete the serial preattentive-cognitive model of human detection, an intermediate, translation step must be performed by determining the "visual information metric" to combine spatial energies over pre-selected regions or over the overall image scene; this metric is essentially a chi-square statistic to determine signal and clutter contributions [2].

Following this, cognitive functions are modeled by [2]:

- implementing a search and detection scheme, to include probabilities of incurring single- and multiple-saccade, or glimpses, for human scan behavior; and finally,
- processing the data using TSD to derive Receiver Operating Characteristic curves to relate detection and false alarm probabilities to time-to-detection.

1.2.2 Models From Transportation

The National Highway Transportation Safety Administration has sponsored the PCDETECT [4] and the Visibility Index and Visibility Index/Fog (VI/FOG) models [5] to assess causes of reduced visibility crashes. The VI/FOG models take environmental considerations such as glare from artificial illumination into consideration, including streetlights, and the PCDETECT model extends that to take into account driver age and glare. Both sets of models are quite simple in formulation and are based on data from the classical Blackwell experiments, which relate differences in visual contrast over a range of illumination conditions [6]. With these classical experiments, the target-background scene is simple: targets are circular, the background is uniform (with considerably less luminance than found outdoors during daylight). The result is a modeling basis on the other extreme of recent theoretical developments in pre-attentive vision described in the previous section. Of important note from the PCDETECT and VI/FOG models is that the key target-to-background discriminant is luminance (i.e., gray scale) contrast. Hence, the fundamental aspect of human vision that is exploited is *contrast sensitivity*. It is precisely this notion, combined with precepts from recent research in human vision, that we develop our "intermediate" applications-oriented model.

2. DEVELOPMENT OF THE MODEL

2.1 Overview

We recognize that the human visual system is tuned to detect not the absolute luminance levels of various areas in a visual scene, but rather the contrast between the luminance levels of adjacent areas. The signal supplied by the eye to the central visual structures does not give equal weight to all regions of the visual scene. Rather, it emphasizes the regions that contain the most information—namely, the regions where there are differences in luminance. Such regions are where our attention is directed when we look

out into the world: they are the most *conspicuous*. Contrast sensitivity, then, underlies our ability to detect objects of interest in the visual scene, and also to discern patterns.

The human visual system is particularly adept and efficient at detecting alternating patterns of light/dark, red/green, and blue/yellow. How well it can detect a particular pattern, i.e., its contrast sensitivity, is a function of that pattern's spatial frequency. To model this aspect of the visual system, we proceed as follows:

1. The given scene is decomposed into three sub-images: a black and white, or light/dark image, an image giving just the reds and greens contained in the scene, and one giving just the blues and yellows.
2. Next, we construct a number of filters, each corresponding to a particular spatial frequency and orientation (rotation) about the line of sight.
3. To each sub-image, we apply each filter, and then weight the result according to the corresponding Contrast Sensitivity Function for that image and filter frequency.
4. Each sub-image is then built back up by pooling these filtered images together.
5. The result of these steps, then***, is what one infers*** the visual system is actually able to discern from the original scene. Each of the three rebuilt sub-images obtained in step 4 will have some average brightness, which is just the average of the brightness of all the pixels making up the image.
6. Each sub-image is then divided into squares, and an average brightness for each of these squares is calculated in the same manner as it was for the overall scene.
7. The ratio of the average brightness of each square (Step 6) to that of the overall sub-image (Step 5) is calculated.
8. A *Scoring Grid* for each sub-image is then constructed from the ratios obtained in Step 7.
9. Finally, an *Overall Scoring Grid* is constructed by combining the scoring grids for the three sub-images (Step 8).

The most conspicuous object in the original scene will lie in the Scoring Grid square whose ratio is the greatest.

2.2 Construction of Subimages

The Black/White, Red/Green, and Blue/Yellow sub-images are next calculated according to the relations

$$\begin{aligned} \text{MonScene} &= \frac{\text{Red} + \text{Blue} + \text{Green}}{3}, \\ \text{RGScene} &= \text{Red} - \text{Green}, \\ \text{BYScene} &= \text{Red} + \text{Green} - 2\cdot\text{Blue}, \end{aligned} \tag{1}$$

Since the individual entries of the RGScene and BYScene arrays can fall outside the 0-1 range as a result of this operation, they are scaled such that their values fall within it. Note that although all values fall in the 0-1 range, a pixel neighborhood with negative contrast feature will simply exhibit local minima in the vicinity of the feature; negative contrast, as such, is not suppressed by our technique. The three sub-images are rendered (drawn) in black and white. For the Red/Green sub-image, white indicates all-red, while black indicates all-green. For the Blue/Yellow sub-image, white indicates all-yellow and black indicates all-blue.

2.3 Construction and Application of Filters

There is evidence to suggest that the human visual system is tuned to the spatial frequencies and rotational orientations listed in Table 1, and we will therefore use these in constructing our filters.

Table 1. Spatial Frequency and Rotational Orientation

SPATIAL FREQUENCY (CYCLES PER DEGREE OF VISUAL ANGLE)	ROTATIONAL ORIENTATION (FROM HORIZONTAL)
$2^{-1} = 0.5000$	0
$2^{-.5} = 0.7071$	$\pi/6$ rad = 30^{o}
$2^{0} = 1.0000$	$2\pi/6$ rad = 60^{o}
$2^{.5} = 1.4142$	$3\pi/6$ rad = 90^{o}
$2^{1} = 2.0000$	$4\pi/6$ rad = 120^{o}
$2^{1.5} = 2.8284$	$5\pi/6$ rad = 150^{o}
$2^{2} = 4.0000$	$6\pi/6$ rad = 180^{o}
$2^{2.5} = 5.6568$	
$2^{3} = 8.0000$	
$2^{3.5} = 11.3137$	
$2^{4} = 16.0000$	
$2^{4.5} = 22.6274$	

For our spatial filter, we use a variant of the Gabor Filter, as described by Watson and Ahumada [7]. Our filter extends over 1^{o} square, chosen to represent *foveal vision*. An alternative and equally valid approach would be to consider *extra-foveal vision*, and to employ correspondingly larger filters of various sizes. In selecting the former case we have implicitly assumed that our observer is attentive, and looking "forward" towards the visual scene. A distracted observer would first have to be drawn to focus on the scene by his or her peripheral, or extra-foveal vision.

Next, we map the 1^{o} square onto a Cartesian coordinate frame. The x and y coordinates of this frame are normalized between –1 and +1 and take on intermediate values corresponding to each pixel within the square. Thus we have created an x- and y-array, with 56 elements whose values are equally spaced between –1 and +1. Since it is desirable to have a coordinate corresponding to zero, we will increase our arrays by one, so they will each have 57 elements. The result is a two-dimensional, 57 x 57 element filter. From these coordinates, we can then obtain a set of rotated coordinates x_{rot} and y_{rot} associated with any counter-clockwise angular rotation (which takes values according to the second column in Table 1) using the standard coordinate transformation

$$x_{rot} = x\cos\psi + y\sin\psi,$$
$$y_{rot} = -x\sin\psi + y\cos\psi. \quad (2)$$

The filter itself takes the form

$$\text{Filter} = e^{-\frac{x_{rot}^2 + y_{rot}^2}{\lambda^2}} \cdot \cos\left(\frac{2\pi\sigma}{dW} x_{rot}\right), \quad (3)$$

where dW is the dimension of our 1^{o} square, ψ is the spatial frequency (which takes values according to the first column in Table 1), and where

$$\lambda = \frac{\rho}{\sigma / dW},$$
$$\rho = \frac{3\sqrt{\log_{10}(2)}}{\pi}. \quad (4)$$

The basis for these parameters is described in [7] referenced above. The units of the cosine's argument in Equ. (3) are

$$\frac{2\pi\frac{\text{radians}}{\text{cycle}}\cdot\sigma\frac{\text{cycles}}{\text{visual degree}}}{\text{dW}\frac{\text{inches}}{\text{visual degree}}}\,x_{\text{rot}}\ \text{inches} = \frac{2\pi\sigma}{\text{dW}}x_{\text{rot}}\ \text{radians},$$

(5)

as required.

The filters can then be applied by convolving them with the visual scene. According to the Convolution Theorem, this is equivalent to taking the Fourier Transforms of the filter and the scene, multiplying them together, and then taking the Inverse Fourier Transform. According to Table 1, we have $12\times7=84$ different filters so our algorithm, applied in Matlab [8] performs 84 convolutions.

2.4 Weighing and Pooling of Filtered Images

We then take both monochromatic and chromatic contrast sensitivity functions (contrast sensitivity *vs* spatial frequency) from Mullen [9] and weight each filtered sub-image by the value of the corresponding contrast sensitivity function for that spatial frequency. These are then *pooled* according to the relation

$$\text{Pooled Sub-Image}_i = \left(\sum_{\sigma}\left[\text{CSF}_i(\sigma)\,\square\,\text{Filtered Sub-Image}_i(\sigma)\right]^{\frac{1}{p}}\right)^p, \tag{6}$$

where

$$i=\begin{cases}1 & \text{Monochrome Sub-Image}\\ 2 & \text{Red/Green Sub-Image}\\ 3 & \text{Blue/Yellow Sub-Image}\end{cases},$$

and where $CSF_i(\sigma)$ is the value of the corresponding Contrast Sensitivity Function at the spatial frequency σ, and p is the *pooling factor*, here taken to be 4. The three pooled sub-images represent the visual information actually taken in at the retina and sent back to the central visual centers in the brain.

2.5 Identification of Conspicuous Elements in the Visual Scene

Our construction work zone scenes are digitized photographs, or *bitmapped images*. Such images are represented in Matlab as three (red *R*, green *G*, and blue *B*) two-dimensional arrays (y pixels high by x pixels wide) overlayed on top of one-another. The elements of each array are unsigned, 8-bit binary integers, ranging from or 0 to 255 decimal. Thus, each pixel can have 256 gradations of red, green, and blue. A value of zero indicates no red (or green or blue), and a value of 255 indicates the brightest or most luminous shade of red (or green or blue). If all three values associated with a particular point are zero, its color would be black (the absence of all color), and if they were all 255, its color would be white (the presence of all colors). If a point's three values were all equal but between 0 and 255, its color would be a shade of gray ranging from black to white. The brightness of a particular point in the picture can thus be obtained by averaging its three *RGB* values. The brightness of the entire scene can be obtained in the same way, by averaging all the values of all the points making it up, and similarly for any portion of the scene. It would be ideal if the images were photometrically correct; however, because our model uses image contrast as opposed to any measure of flux density, the only necessary assumption is that any two (say, before and after scenes) images retain the same relative calibration. This requirement can usually be met, for example, by using the same camera to capture the images.

2.6 Determining the Scoring Grid

To determine a Scoring Grid, which allows us to rank order most- to least-conspicuous 1^o pixel elements within a scene, we first define the Contrast Ratio of the i^{th} square as

$$\text{Contrast Ratio}_{\text{Square i}} = \frac{\text{Brightness}_{\text{Square i}}}{\text{Brightness}_{\text{Entire Scene}}}. \quad (7)$$

A Contrast Ratio (CR) near zero indicates that a square is darker than the overall scene, while a CR larger than one indicates the square is brighter. A CR of one indicates that a particular square is as bright as the overall scene, and hence does not contrast with it. The farther a CR is from one, the more it contrasts with the surrounding scene and the more conspicuous it is. The lighter an individual square, the more conspicuous it is, and the darker a square, the less conspicuous it is. Denoting CR to be the CR array (with 1^o square elements),

$$CR' = |CR - 1| \quad (8)$$

Examining $CR - 1$, we see that $-1 \le CR - 1 \le \infty$, and $CR - 1 = 0$ corresponds to no contrast. Thus, $0 \le CR' \le \infty$ and $CR' = 0$ corresponds to no contrast. We observe that CR' cannot tell us whether a particular square is lighter or darker than the overall scene, only that it is different. (This gives us relative conspicuity within a scene but not between scenes.) We cannot render CR', since it is not within the range of zero to one. We can, however, calculate a normalized array CR_{norm} that does fall within this range according to the relation

$$CR_{norm} = \frac{CR' - \min(CR')}{\max\left[CR' - \min(CR')\right]}. \quad (9)$$

In words, we first shifted CR' so that its smallest element is zero [the numerator of Eq.(9)]. We then divided by the maximum element of this resulting array so that now the largest element is one [the denominator of Eq. (9). Next, we make all the elements associated with a particular square equal to CR_{norm} for that square. The squares will then render as varying shades of gray, and there will always be at least one completely black square, corresponding to the portion of the overall scene having the *least* [not necessarily zero, because of Eq.(9)] contrast. Likewise, there will always be at least one completely white square, corresponding to the portion of the overall scene having the greatest contrast. Hence, with CR', we have developed a *Scoring Grid* array to identify the most conspicuous elements of a particular scene.

There is no known physiological basis for the Scoring Grid concept. We have created it with the goal of methodically and consistently picking out the most conspicuous element(s) in a given scene. The object of interest can occupy any portion of a visual scene—from a very small part to a very large part. If we size our squares too small our scoring grid may identify many different "most conspicuous objects" scattered throughout the scene. If we size the squares too large, the most conspicuous object may get "averaged" into the background when the intensity of the square containing it is calculated.

2. VERIFICATION OF THE MODEL

To verify our computational vision model, we use the monochromic, sinusoidally varying pattern damped exponentially in both the horizontal and vertical_directions, superimposed on a uniform field of "background noise". This is shown in Figure 1. The pattern is a variant of a two-dimensional Gabor Function (described in [7]), and given by

$$G(x,y) = I\left\{e^{-\left(\frac{x}{\lambda}\right)^2}\cos\left[2\pi\left(\frac{\sigma}{dW}\right)x\right]\right\}\left\{e^{-\left(\frac{y}{\lambda}\right)^2}\cos\left[2\pi\left(\frac{\sigma}{dW}\right)y\right]\right\}, \quad (10)$$

where the amplitude I and the spatial frequency σ are chosen to be

$$I = 1,$$

$$\sigma = .5\frac{\text{Cycles}}{\text{Degree of Visual Angle}},$$

and where ρ and λ are as defined in the previous section. As before, dW is the dimension (in this case 53 pixels) of a square 1^o of visual angle to a side, as viewed on a monitor by an observer approximately 0.8

meters in front. The values x and y (not to be confused with x and y as used in the previous section) are the coordinates (also in pixels) associated with the scene, adjusted so that the point (0,0) corresponds to its center.

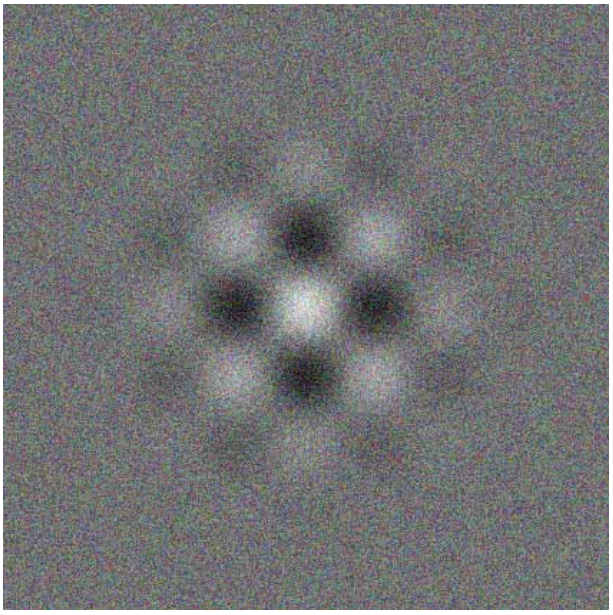

Figure 1. Gabor Pattern Superimposed on a Uniform Field of Noise

Because the form of this pattern corresponds to that of our filters, we should very nearly recover the monochrome sub-image in our analysis by reconstructing the B/W subimage via the reconstructed R/G and B/Y subimages. That is precisely what we have done with Figure 2. The images are close – as is the overall scoring grid, shown in Figure 3. This indicates that indeed input patterns can be reconstructed via computational process of our model.

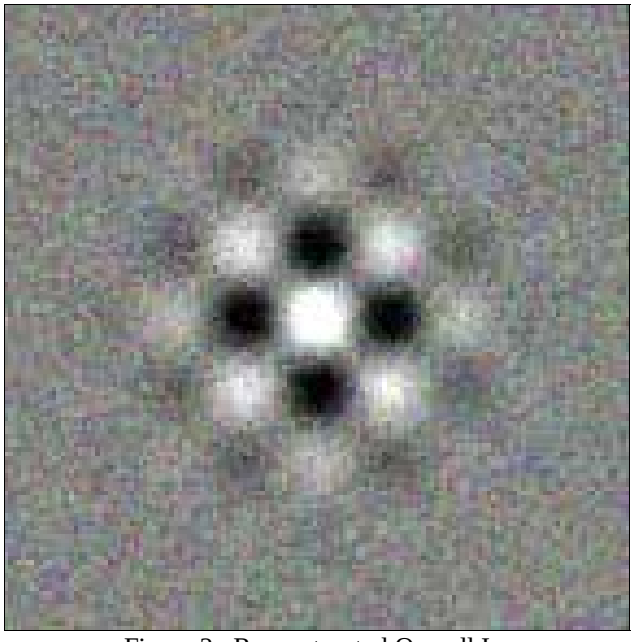

Figure 2. Reconstructed Overall Image

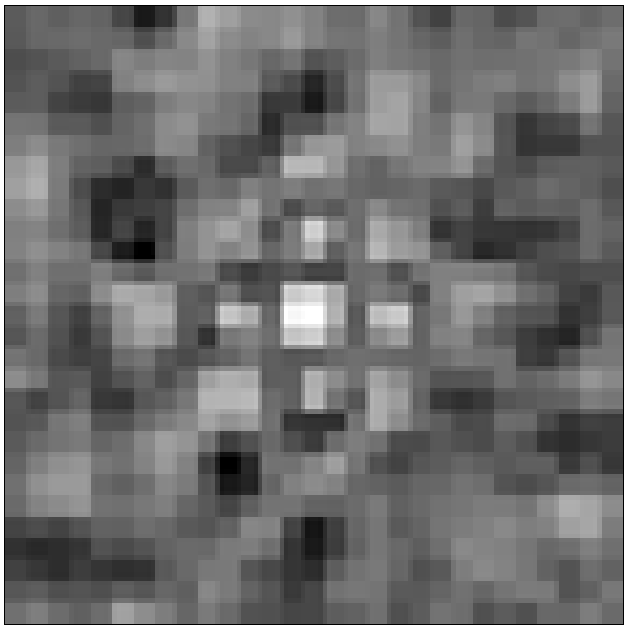

Figure 3. Reconstructed Overall Scoring Grid

3. APPLICATION TO ROADSIDE 'WORK ZONE' SCENE

A typical cluttered roadway scene shown in Figure 4 is analyzed using our computational vision model, but with the final "Scoring Grid" result shown in Figure 5. From the Scoring Grid, high contrast and bright elements of the scene (e.g., taillights, striping, Caltrans tow truck, construction warning sign, bright clouds) are most conspicuous, as we would expect.

Figure 4. Original Image Subdivided

Figure 5. Original Image and Corresponding Overall Scoring Grid

Figure 6 shows results from performing the same analysis on a simpler scene with a bright lime-green circle inserted the scene, as shown. The Scoring Grid indicates that the circle is more conspicuous than the workman's vest, a result that makes intuitive sense. The circle is considerably brighter than the vest in both the Red/Green and Blue/Yellow sub-images (not shown). Neither it, nor the vest, seems to be able to compete with the sky in the Black/White sub-image, and here they appear to be equally bright.) One insight into making an object more conspicuous, therefore, is to increase its conspicuity in all three of the visual "channels" — the Black/White, Red/Green, and Blue/Yellow. Lime-green appears to do a better job of this than orange.

Figure 6. Image with Lime-Green Circle Superimposed and Corresponding Scoring Grid

Going in the other direction, we make the vest the same color as the shaded grass immediately behind the workman and show the results in Figure 7. The workman almost disappears from the scene, and the most conspicuous elements in the scene become the sky above the workman and the lighted ground to front and to the left.

Figure 7. Image with Darkened Vest Superimposed and Corresponding Scoring Grid

4. CONCLUSIONS AND NEXT STEPS

We have developed, validated and implemented an efficient algorithm to identify the conspicuous elements in a visual scene, based on the human visual system's contrast sensitivity function. A "scoring grid" has been devised to view quickly and easily the results of the computations. Actual, numerical values associated with the conspicuity of any element in the scene were performed. The algorithm is coded in Matlab and available to any researcher or transportation safety professional [10]. It has been delivered to the California State Department of Transportation.

However, the work to date should only be viewed as a first step. A number of refinements and extensions are possible and would seem to be desirable:

1. Here we assumed an "attentive" driver, and modeled foveal vision. By increasing the size of our filters and adding additional logic we can model extra-foveal (peripheral) vision and test the ability of various visual schemes to alert inattentive drivers.

2. In quantifying conspicuity, we have compared the elements in a visual scene against a background consisting of the entire scene. This represents an observer's "first glance" at a visual scene, where we assume the driver will focus on the most conspicuous element overall. It would also be desirable to model the observer's "second pass" at the scene, in which the driver quickly scans the scene for other elements that stand out from their *immediate* surroundings. Depending upon what else is in the scene, this activity could enhance or detract from the driver's efforts.

3. We have limited our attention to still scenes. Contrast sensitivity also includes sensitivity to movement, which can be modeled in a manner quite similar to that of the still case. By incorporating sensitivity to movement, we can then assess the conspicuity of schemes that add movement (or a sense of movement) to important elements in the scene.

4. With the addition of a faster convolution routine, we believe that we can make our computational algorithm real-time. Given that, with further development, we conceive of a field-portable "conspicuity meter" to be used by traffic safety practitioners or even work zone crews.

Whether we achieved our initial objectives of a "middle ground", where a relatively computationally efficient model can provide answers will likely be fully answered with further research as suggested above. Moreover, higher level objectives such as time, dollar savings and improved safety can be realized only after such improvements are made, our technique is converted into an operational tool, and further applications are undertaken and evaluated.

ACKNOWLEDGMENTS

This work was performed as part of the California PATH Program of the University of California in cooperation with the State of California Business, Transportation and Housing Agency, Department of Transportation. The authors thank Professor Stanley A. Klein, and to PhD Candidate Laura Walker of the Graduate Group in Vision Science, University of California at Berkeley and Aaron Steinfeld of California PATH for their generous advice and assistance.

REFERENCES

1 Doll, J. et. al., "Target and background characterization based on a simulation of human pattern perception," *Proceedings, SPIE Characterization, Propagation, and Simulation of Sources and Backgrounds III*, pp. 432 - 454, 1993.

2 Witus, G. et. al., "Evaluating an Army camouflaged vehicle visual signature model for measuring civilian vehicle conspicuity," *General Motors Publication R&D-8350,* May 1995.

3 Meitzler, T. et. al., “Adapting an Army vision model for measuring armored-vehicle camouflage to evaluating the conspicuity of civilian vehicles: preliminary results of a joint army-general motors project,” *General Motors Publication R&D-8244,* Jan. 1995.
4 Farber, E. and Matle, C., PCDETECT: a revised version of the detect seeing distance model, Paper No 880546, Presented at the TRB 68th Annual Meeting, 1989.
5 Tijerina, L., et. Al. “Examination of reduced visibility crashes and potential IVHS countermeasures,” (DOT HS 808 201). Washington D.C.: U.S. Department of Transportation, Jan. 1995.
6 Blackwell, H.R., “Contrast thresholds of the human eye,” *Journal of the Optical Society of America,* 1946, Volume 36, pp. 624-643.
7 Watson, A.B., and Ahumada, A.J. “Model of human vision-motion sensing,” *Journal of the Optical Society of America,* 1985, Volume 2, No. 2, pp. 328-329.
8 http://www.mathworks.com/products/matlab/
9 Mullen, K.T., “The contrast sensitivity of human colour vision to red-green and blue-yellow chromatic gratings, *Journalof Physiology,* 1985, Vol. 359, pp. 381-400.
10 Barton, J.E., and Misener, J.A., “Roadway and work crew conspicuity,” (California PATH Research Report UCB-ITS-PRR-2000-23). UC Berkeley: Dec., 2000.